SCIENCE CHINA
Information Sciences

• RESEARCH PAPER •

December 2023, Vol. 66 222306:1–222306:13
https://doi.org/10.1007/s11432-022-3832-6

Transformation of a metasurface on the substrate interface into the same metasurface in a homogenized substrate based on two kinds of modified Babinet's principles

Xiaobo LIU[1,2†], Rui LU[1†], Anxue ZHANG[1], Qiang CHENG[3*] & Xiaoming CHEN[1*]

[1]*School of Information and Communications Engineering, Xi'an Jiaotong University, Xi'an* 710049*, China;*
[2]*School of Mathematics and Statistics, Xi'an Jiaotong University, Xi'an* 710049*, China;*
[3]*State Key Laboratory of Millimeter Waves and School of Electrical Engineering, Southeast University, Nanjing* 210096*, China*

Received 20 November 2022/Revised 8 March 2023/Accepted 23 July 2023/Published online 2 November 2023

Abstract Previously, the metasurface was usually manufactured on a dielectric substrate using the printed circuit boards (PCB) technology. However, due to the existence of the substrate interface, the electromagnetic radiation and coupling of the sub-wavelength metasurface becomes more complex for theoretical analysis. To this end, an indirect method is developed to transform the problem of a metasurface in a dielectric half-space into a simpler problem of the same metasurface in a homogenized dielectric space. Specifically, two different theoretical models of complementary metasurfaces in a dielectric half-space are first given. A specific yet unknown relative permittivity is included in one model to realize the above transformation. By comparing these two theoretical models in terms of the surface impedance matrix, the specific yet unknown relative permittivity is analytically derived as $\sqrt{\epsilon_{r,\mathrm{unk}}} = \sqrt{\epsilon_{r,1}}/2 + \sqrt{\epsilon_{r,2}}/2$. Finally, two arbitrary metasurfaces are given to verify the proposed theory for arbitrary incidence wave in dielectric half-space. The theory can greatly simplify the analysis and design of the metasurface in a dielectric halfspace, because only the metasurface in a homogenized dielectric space like vacuum needs to be theoretically solved after completing the above transformation.

Keywords dielectric half-space, homogenized dielectric space, metasurface, relative permittivity, surface impedance matrix, substrate interface

Citation Liu X B, Lu R, Zhang A X, et al. Transformation of a metasurface on the substrate interface into the same metasurface in a homogenized substrate based on two kinds of modified Babinet's principles. Sci China Inf Sci, 2023, 66(12): 222306, https://doi.org/10.1007/s11432-022-3832-6

1 Introduction

The metasurface is composed of periodic sub-wavelength metallic elements [1, 2]. Due to the unique periodicity of the metallic structure, the metasurface can be employed to realize various devices with superior performances, such as polarization converters [3–8], filters [9–11], cloaks [12–15], and metagratings [16–21]. Besides numerous application-oriented designs of metasurfaces, much attention has been paid to the electromagnetic theories of the metasurface. Since the metasurface is usually manufactured on a dielectric substrate using the printed circuit boards (PCB) technology, it is highly desirable to solve the boundary condition of the metasurface on the substrate interface.

According to the previous study, when the periodicity is much smaller than the operation wavelength, the metasurface can be regarded as a homogenized surface with surface impedance (matrix) in the network transmission theory [22, 23]. To this end, many methods have been developed to solve the metasurface on the substrate interface. (1) The first kind of method is the equivalent RLC (resistance, inductance,

* Corresponding author (email: qiangcheng@seu.edu.cn, xiaoming.chen@mail.xjtu.edu.cn)
† Liu X B and Lu R have the same contribution to this work.

and capacitance) circuit method [24–27]. According to the method, the metasurface is equivalent to the capacitance and inductance related to the metallic elements and substrate. However, due to the physical ambiguity of equivalent capacitance and inductance, these electrical parameters are always solved through the numerical fitting rather than the analytical solution. Thus, the method makes great progress in partial metasurfaces, but it is restricted by the difficulty in obtaining solutions to these electrical parameters. (2) The second kind of methods is the average boundary condition method [28–34]. In the method, the surface impedance (matrix) actually corresponds to the average electrical field and current. It should be noted that these electrical fields and currents must satisfy the boundary condition of the metasurface. To this end, researchers need to analyze the electromagnetic radiation and coupling of the sub-wavelength metallic element on the substrate interface. However, due to the influence of the dielectric interface, the electromagnetic radiation and coupling of the sub-wavelength metallic elements become highly complex, which results in difficulty in solving the electromagnetic fields for the metasurface on the substrate interface. (3) Finally, some numerical methods like the method of moments (MoMs) can be also applied for the problem [35, 36]. Similar to software simulations, these numerical methods hold valid for the metasurface, but there is still room for improvement in the influence of the substrate interfaces. For example, the scalar function $\mathrm{e}^{-\mathrm{j}k_0 r}/4\pi r$ is applied for the current radiation in vacuum for the MoMs. When the metasurface is placed in the homogenized medium like air, only the induced current on the metallic element needs to be considered. However, when the metallic element is placed on the substrate interface like air and FB4 substrates, the FB4 substrate needs to be regarded as air with the polarization current for the scalar function $\mathrm{e}^{-\mathrm{j}k_0 r}/4\pi r$, which obviously increases the difficulty in acquiring the solution for the boundary condition of the metasurface. Thus, it can be concluded that, due to the existence of the substrate interface, the boundary condition of the metasurface becomes more complex than the case in vacuum for many existing methods.

Here, an alternative approach is given to simplify the problem. For example, we can try to convert the metasurface on the substrate interface into the same metasurface in a homogenized medium (Note that the homogeneous medium is not the equivalent one of the metasurface [37]), so that the above analysis methods like MoMs will easily hold valid. Specifically, in our previous work [38], we introduced a kind of zero-thickness homogeneous media for complementary metasurfaces on the substrate interface. More importantly, it is then found that this kind of zero-thickness homogeneous media can have the problem of the metasurface on the substrate interface transformed into another problem of the same metasurface in a homogenized media. If so, the problem of the metasurface on the substrate interface can be greatly simplified after completing the above transformation, because only the metasurface in a homogenized media like vacuum needs to be theoretically solved. However, the specific yet unknown relative permittivity of the homogeneous medium remained to be solved, which exactly transforms a metasurface on the substrate interface into the same metasurface in a homogenized media.

In this work, we provide a solid mathematical and physical foundation to solve the above specific yet unknown relative permittivity of the zero-thickness homogeneous medium covering the metasurface on the substrate interface. Firstly, two theoretical models of Babinet's principle are given for complementary metasurfaces in a dielectric half-space. One model can realize the above transformation with an unknown relative permittivity $\epsilon_{r,\mathrm{unk}}$, and the other does not include arbitrary unknown parameter. Then, two theoretical models are combined to solve the unknown relative permittivity as $\sqrt{\epsilon_{r,\mathrm{unk}}} = \sqrt{\epsilon_{r,1}}/2+\sqrt{\epsilon_{r,2}}/2$. Finally, two examples are given to verify the theory, where the boundary condition of the metasurface in the homogeneous medium is converted into that on the substrate interface. Compared to the existing methods for metasurface in the homogeneous medium, the study does not directly solve the boundary condition of the metasurface on the substrate interface, but reveals how to transform a complex problem of metasurface on the substrate interface into another simple problem of the same metasurface in a homogenized media. Thus, the proposed method provides an alternative theoretical approach to simplify the problem of the metasurface on the substrate interface.

The rest of the paper is organized as follows. In Section 2, two theoretical models of complementary metasurfaces in a dielectric half-space are given. In Subsection 3.1, the concept of the surface impedance matrix is introduced to simplify these two models. In Subsections 3.2 and 3.3, the two theoretical models are rewritten in terms of their surface impedance matrices. In Subsection 3.4, the specific yet unknown relative permittivity is analytically solved by comparing these two models with each other. In Subsection 4.1, we provide the verification process for the proposed theory. In Subsections 4.2 and 4.3, we use two different kinds of metasurfaces to support the proposed theory, regardless of the substrate and incidence angle. Finally, Section 5 presents the conclusion drawn from this study.

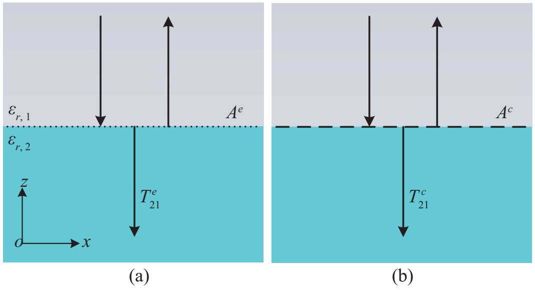

Figure 1 (Color online) Original model in a dielectric half-space for (a) metasurface A^e and (b) complementary metasurface A^c.

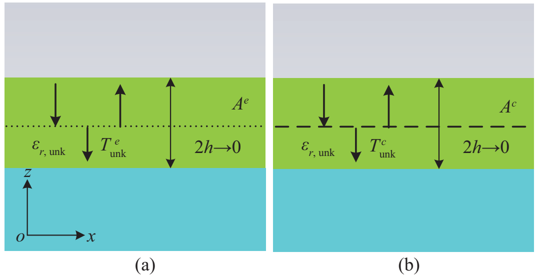

Figure 2 (Color online) Updated model in a dielectric half-space for (a) metasurface A^e and (b) complementary metasurface A^c.

2 Theoretical basis

In this section, we find a way to transform the problem of a metasurface between two different media to the same metasurface in a homogeneous medium which includes the information of the two original media. Specifically, as shown in Figure 1, two complementary metasurfaces A^e and A^c are placed on the interface between dielectrics 1 and 2. When a x- or y-polarized wave with an electrical field $\boldsymbol{E}_{\mathrm{inc}}$ impinges onto A^e, the transmitted electrical field is denoted as $\boldsymbol{E}_{\mathrm{tra}}$, and the corresponding matrix is denoted as $\boldsymbol{T}^e_{21}$, i.e., $\boldsymbol{E}_{\mathrm{tra}} = \boldsymbol{T}^e_{21}\boldsymbol{E}_{\mathrm{inc}}$, where the subscript "21" indicates that the wave impinges from dielectric 1 to dielectric 2. Similarly, $\boldsymbol{T}^c_{21}$ is defined as the corresponding tangential transmission matrix for A^c. In order to establish the relationship between $\boldsymbol{T}^e_{21}$ and $\boldsymbol{T}^c_{21}$, the metasurface in a dielectric half-space can be regarded to be embedded into a homogenized dielectric layer with a specific yet unknown relative permittivity $\epsilon_{r,\mathrm{unk}}$, as shown in Figure 2 (Note that the specific yet unknown relative permittivity $\epsilon_{r,\mathrm{unk}}$ is not the equivalent permittivity of the three-dimensional metamaterial [37]). As the thickness of such an unknown homogenized dielectric layer approaches zero, the updated model (cf. Figure 2) boils down to the original model (cf. Figure 1). According to the model, the relationship between A^e and A^c can be established through the process $\boldsymbol{T}^e_{21} \Rightarrow \boldsymbol{T}^e_{\mathrm{unk}} \Rightarrow \boldsymbol{T}^c_{\mathrm{unk}} \Rightarrow \boldsymbol{T}^c_{21}$ as follows [28] (For better comparison with the second model, only the normal incidence is considered in the following equations, which can be also extended to the general arbitrary oblique incidence):

$$(\boldsymbol{T}^e_{21})^{-1} = (\boldsymbol{t}_{\mathrm{unk},1})^{-1}\boldsymbol{t}_{1,\mathrm{unk}}\left[(\boldsymbol{T}^e_{\mathrm{unk}})^{-1} - 2\boldsymbol{U} + (\boldsymbol{t}_{1,\mathrm{unk}})^{-1} + (\boldsymbol{t}_{2,\mathrm{unk}})^{-1}\right], \tag{1}$$

$$\boldsymbol{U} = \boldsymbol{T}^e_{\mathrm{unk}} - Z^2_{\mathrm{unk}}\boldsymbol{Z}^{-1}_{c,\mathrm{unk}}\boldsymbol{T}^c_{\mathrm{unk}}\boldsymbol{Z}^{-1}_{c,\mathrm{unk}}, \tag{2}$$

$$(\boldsymbol{T}^c_{21})^{-1} = (\boldsymbol{t}_{\mathrm{unk},1})^{-1}\boldsymbol{t}_{1,\mathrm{unk}}\left[(\boldsymbol{T}^c_{\mathrm{unk}})^{-1} - 2\boldsymbol{U} + (\boldsymbol{t}_{1,\mathrm{unk}})^{-1} + (\boldsymbol{t}_{2,\mathrm{unk}})^{-1}\right], \tag{3}$$

with

$$\begin{aligned} \boldsymbol{Z}_{c,\mathrm{unk}} &= Z_{\mathrm{unk}}\begin{bmatrix} 0 & -1 \\ 1 & 0 \end{bmatrix}, \quad \boldsymbol{t}_{\mathrm{unk},1} = \left\{\frac{Z_{\mathrm{unk}} - Z_1}{Z_{\mathrm{unk}} + Z_1} + 1\right\}\boldsymbol{U}, \\ \boldsymbol{t}_{1,\mathrm{unk}} &= \left\{\frac{Z_1 - Z_{\mathrm{unk}}}{Z_{\mathrm{unk}} + Z_1} + 1\right\}\boldsymbol{U}, \quad \boldsymbol{t}_{2,\mathrm{unk}} = \left\{\frac{Z_2 - Z_{\mathrm{unk}}}{Z_{\mathrm{unk}} + Z_2} + 1\right\}\boldsymbol{U}, \end{aligned} \tag{4}$$

where $\boldsymbol{T}^e_{\mathrm{unk}}$ is the tangential transmission matrix for A^e in the homogenized dielectric layer; $\boldsymbol{U}$ is a 2×2 identity matrix; $Z_{\mathrm{unk}} = \sqrt{\frac{\mu_0}{\epsilon_0\epsilon_{r,\mathrm{unk}}}}$ is the wave impedance of the unknown homogenized dielectric, and other wave impedances like Z_1 and Z_2 can be similarly defined as Z_{unk}. It should be noted that these inverse matrices should exist due to their clear physical meanings. For example, in the equation of $\boldsymbol{E}_{\mathrm{tra}} = \boldsymbol{T}^e_{21}\boldsymbol{E}_{\mathrm{inc}}$, $\boldsymbol{T}^e_{21}$ relates the incident field to the transmitted field at the interface of the metasurface, and these fields should have finite values. If the inverse of the original matrix $\boldsymbol{T}^e_{21}$ does not exist, the determinant of the original matrix should be (nearly) equal to zero, i.e., $|\boldsymbol{T}^e_{21}| \to 0$. Further, the determinant of the inverse matrix should (nearly) approach infinity, i.e., $|\boldsymbol{T}^e_{21}|^{-1} \to \infty$, which will yield an infinite field for the metasurface. Thus, these inverse matrices should physically exist.

Note that Eq. (1) indicates that a specific yet unknown $\epsilon_{r,\mathrm{unk}}$ can have the problem $\boldsymbol{T}^e_{21}$ of the metasurface in a dielectric half-space transformed into another problem $\boldsymbol{T}^e_{\mathrm{unk}}$ of the metasurface in a homogenized dielectric, which can be applied to reduce the difficulty in solving the metasurface's boundary condition

(It should be noted that, the study is aimed at $\epsilon_{r,\mathrm{unk}}$ to realize the transformation between $\boldsymbol{T}_{21}^{e}$ and $\boldsymbol{T}_{\mathrm{unk}}^{e}$ rather than the solution of the specific metasurface). However, since the model does not directly break the existing Babinet's principle, it cannot give the theoretical value of the unknown relative permittivity beforehand (Through multiple trials and analogies, we assumed its value as $\epsilon_{r,1}/2+\epsilon_{r,2}/2$ in [38,39], while it will be theoretically verified that the value satisfies the equation $\sqrt{\epsilon_{r,\mathrm{unk}}}=\sqrt{\epsilon_{r,1}}/2+\sqrt{\epsilon_{r,2}}/2$ in Section 3). Thus, an open problem remains to be solved about the specific yet unknown relative permittivity $\epsilon_{r,\mathrm{unk}}$.

In order to solve the problem, another model of the modified Babinet's principle is proposed for complementary metasurfaces A^e and A^c in a dielectric half-space. According to the theory, their tangential transmission matrices will satisfy the following equations at normal incidence [40]:

$$2Z_2^2(\boldsymbol{T}_{21}^{c})^{-1}=2\boldsymbol{Z}_{c,1}(\boldsymbol{T}_{21}^{e}-\boldsymbol{t}_{21})^{-1}\boldsymbol{Z}_{c,2}+\left(Z_2^2-Z_1^2\right)\boldsymbol{U},\tag{5}$$

with

$$\boldsymbol{Z}_{c,l}=Z_l\boldsymbol{K}=Z_l\begin{bmatrix}0&-1\\1&0\end{bmatrix},\quad \boldsymbol{t}_{21}=\left(\frac{Z_2-Z_1}{Z_2+Z_1}+1\right)\boldsymbol{U}.\tag{6}$$

Since the theory is established based on the modified Babinet's principle, $\epsilon_{r,\mathrm{unk}}$ does not appear in (5). Especially, it should be noted that the above theory can also give the general relationship between $\boldsymbol{T}_{21}^{e}$ and $\boldsymbol{T}_{21}^{c}$ at oblique incidence, but it only has high accuracy at small incidence angles. Therefore, only the normal incidence is considered for the above theory.

Finally, due to the unique reflection and transmission characteristics of the metasurface, these two theoretical models should be consistent with each other at normal incidence. By combining two kinds of theoretical models, one can analytically solve the specific yet unknown relative permittivity $\epsilon_{r,\mathrm{unk}}$. More importantly, the problem of the metasurface in a dielectric half-space can be transformed into another problem of the same metasurface in a homogenized dielectric.

3 Solution of the unknown relative permittivity

In this section, two theoretical models about complementary metasurfaces will be expressed in terms of the surface impedance matrix. By comparing these two models, the unknown relative permittivity $\epsilon_{r,\mathrm{unk}}$ can be analytically derived. Finally, based on the proposed theory, the problem of the metasurface in a dielectric half-space can be accurately converted into a simpler problem of the same metasurface in a homogenized dielectric with a relative permittivity of $\epsilon_{r,\mathrm{unk}}$.

3.1 Relationship between tangential transmission matrix and surface impedance matrix

In order to solve the unknown relative permittivity $\epsilon_{r,\mathrm{unk}}$, these two theoretical models need to be combined together. However, due to their complex mathematical forms, it is hard to directly compare them with each other. In this case, considering the tangential transmission matrix actually depends on the incidence dielectric like $\boldsymbol{T}_{21}^{e}\neq\boldsymbol{T}_{12}^{e}$, the surface impedance matrix (which is symmetric about the incidence substrate like $\boldsymbol{Z}_{21}^{e}=\boldsymbol{Z}_{12}^{e}$ in (10)) is introduced to replace the tangential transmission matrix for convenience. Thus, these two kinds of Babinet's principles will be rewritten in terms of these surface impedance matrices for comparison.

Firstly, when a wave with a tangential electrical field $\boldsymbol{E}_{\mathrm{inc}}$ impinges onto the metasurface A^e in a dielectric half-space, the corresponding transmitted electrical field is denoted as $\boldsymbol{E}_{\mathrm{tra}}$. Thereby, the transmission matrix $\boldsymbol{T}_{21}^{e}$ is given as follows [27]:

$$\boldsymbol{E}_{\mathrm{tra}}=\boldsymbol{T}_{21}^{e}\boldsymbol{E}_{\mathrm{inc}}=\left(\boldsymbol{U}-\boldsymbol{Z}_{||,21}\boldsymbol{I}_{21}^{e}\right)\boldsymbol{t}_{21}\boldsymbol{E}_{\mathrm{inc}},\tag{7}$$

with

$$\boldsymbol{Z}_{||,21}=\frac{Z_1Z_2}{Z_2+Z_1}\boldsymbol{U},\tag{8}$$

where $\boldsymbol{I}_{21}^{e}$ is the induction matrix relating the external excited field $\boldsymbol{t}_{21}\boldsymbol{E}_{\mathrm{inc}}$ to the induced surface current density $\boldsymbol{J}_{21}^{e}$, i.e., $\boldsymbol{J}_{21}^{e}=\boldsymbol{I}_{21}^{e}\boldsymbol{t}_{21}\boldsymbol{E}_{\mathrm{inc}}^{\tan}$; the radiation matrix $\boldsymbol{Z}_{||,21}$ describes the relationship between the induced surface current density $\boldsymbol{J}_{21}^{e}$ and the secondary re-radiated wave from the metasurface.

Secondly, the surface impedance matrix $\boldsymbol{Z}^e_{21}$ is introduced here to describe the relationship between the total electrical field $\boldsymbol{E}_{\rm tra}$ and the induced surface current density $\boldsymbol{J}^e_{21}$ on the metasurface as follows:

$$\boldsymbol{E}_{\rm tra} = \boldsymbol{Z}^e_{21}\boldsymbol{J}^e_{21} = \boldsymbol{Z}^e_{21}\boldsymbol{I}^e_{21}\boldsymbol{t}_{21}\boldsymbol{E}_{\rm inc}. \tag{9}$$

Finally, by comparing (7) and (9), $\boldsymbol{I}^e_{21}$ can be expressed in terms of $\boldsymbol{Z}^e_{21}$ as follows:

$$\boldsymbol{I}^e_{21} = \left(\boldsymbol{Z}^e_{21} + \boldsymbol{Z}_{||,21}\right)^{-1}, \quad \boldsymbol{Z}^e_{21} = \boldsymbol{Z}^e_{12}, \tag{10}$$

where $\boldsymbol{I}^e_{21} = \boldsymbol{I}^e_{12}$ has been previously verified in [20]. Thereby, $\boldsymbol{T}^e_{21}$ can be represented in terms of $\boldsymbol{Z}^e_{21}$ by inserting (9) into (7) as follows:

$$\boldsymbol{T}^e_{21} = \boldsymbol{Z}^e_{21}\boldsymbol{I}^e_{21}\boldsymbol{t}_{21} = \boldsymbol{Z}^e_{21}\left(\boldsymbol{Z}^e_{21} + \boldsymbol{Z}_{||,21}\right)^{-1}\boldsymbol{t}_{21}, \tag{11}$$

$$\boldsymbol{T}^e_{21} - \boldsymbol{t}_{21} = -\boldsymbol{Z}_{||,21}\boldsymbol{I}^e_{21}\boldsymbol{t}_{21} = \boldsymbol{Z}_{||,21}\left(\boldsymbol{Z}^e_{21} + \boldsymbol{Z}_{||,21}\right)^{-1}\boldsymbol{t}_{21}, \tag{12}$$

with

$$\boldsymbol{T}^c_{21} = \boldsymbol{Z}^c_{21}\boldsymbol{I}^c_{21}\boldsymbol{t}_{21} = \boldsymbol{Z}^c_{21}\left(\boldsymbol{Z}^c_{21} + \boldsymbol{Z}_{||,21}\right)^{-1}\boldsymbol{t}_{21}, \tag{13}$$

$$\boldsymbol{T}^c_{21} - \boldsymbol{t}_{21} = -\boldsymbol{Z}_{||,21}\boldsymbol{I}^c_{21}\boldsymbol{t}_{21} = -\boldsymbol{Z}_{||,21}\left(\boldsymbol{Z}^c_{21} + \boldsymbol{Z}_{||,21}\right)^{-1}\boldsymbol{t}_{21}, \tag{14}$$

where Eqs. (13) and (14) are resulted from a similar operation for $\boldsymbol{Z}^c_{21}$ and $\boldsymbol{T}^c_{21}$. Obviously, based on (11)–(14), Eq. (5) of the modified Babinet's principle can be successfully rewritten in terms of the surface impedance matrices $\boldsymbol{Z}^e_{21}$ and $\boldsymbol{Z}^c_{21}$.

Except for the second modified Babinet's principle, Eqs. (1)–(3) have not been rewritten due to the tangential transmission matrices $\boldsymbol{T}^e_{\rm unk}$ and $\boldsymbol{T}^c_{\rm unk}$. When the metasurface A^e (A^c) is placed in the homogenized dielectric with $\epsilon_{r,{\rm unk}}$, the relationship between the tangential transmission matrix $\boldsymbol{T}^e_{\rm unk}$ ($\boldsymbol{T}^c_{\rm unk}$) and the corresponding surface impedance matrix $\boldsymbol{Z}^e_{\rm unk}$ ($\boldsymbol{Z}^c_{\rm unk}$) can be similarly rewritten as follows:

$$\boldsymbol{T}^e_{\rm unk} = \boldsymbol{Z}^e_{\rm unk}(\boldsymbol{Z}^e_{\rm unk} + \boldsymbol{Z}_{||,{\rm unk}})^{-1}, \tag{15}$$

$$\boldsymbol{T}^e_{\rm unk} - \boldsymbol{U} = -\boldsymbol{Z}_{||,{\rm unk}}(\boldsymbol{Z}^e_{\rm unk} + \boldsymbol{Z}_{||,{\rm unk}})^{-1}, \tag{16}$$

$$\boldsymbol{T}^c_{\rm unk} = \boldsymbol{Z}^c_{\rm unk}(\boldsymbol{Z}^c_{\rm unk} + \boldsymbol{Z}_{||,{\rm unk}})^{-1}, \tag{17}$$

$$\boldsymbol{T}^c_{\rm unk} - \boldsymbol{U} = -\boldsymbol{Z}_{||,{\rm unk}}(\boldsymbol{Z}^c_{\rm unk} + \boldsymbol{Z}_{||,{\rm unk}})^{-1}, \tag{18}$$

with

$$\boldsymbol{t}_{\rm unk} = \boldsymbol{U}, \quad \boldsymbol{Z}_{||,{\rm unk}} = \frac{Z_{\rm unk}}{2}\boldsymbol{U}, \tag{19}$$

where $\boldsymbol{t}_{\rm unk}$ is the tangential transmission matrix in a homogenized dielectric without metasurface. Finally, based on (11)–(18), Eqs. (1)–(3) can also be rewritten as the relationship between $\boldsymbol{Z}^e_{21}$ and $\boldsymbol{Z}^c_{21}$ through the process $\boldsymbol{Z}^e_{21}(\boldsymbol{T}^e_{21}) \Rightarrow \boldsymbol{Z}^e_{\rm unk}(\boldsymbol{T}^e_{\rm unk}) \Rightarrow \boldsymbol{Z}^c_{\rm unk}(\boldsymbol{T}^c_{\rm unk}) \Rightarrow \boldsymbol{Z}^c_{21}(\boldsymbol{T}^c_{21})$.

3.2 The first model in terms of the surface impedance matrix

Here, the surface impedance matrices will be introduced for the first theoretical model with an unknown relative permittivity $\epsilon_{r,{\rm unk}}$.

Firstly, based on (4) and the equation $Z^2_{\rm unk}\boldsymbol{Z}^{-1}_{c,{\rm unk}}\boldsymbol{Z}^{-1}_{c,{\rm unk}} = -\boldsymbol{U}$, Eqs. (1)–(3) can be rewritten as follows:

$$(\boldsymbol{T}^e_{21})^{-1} = \frac{Z_1}{Z_{\rm unk}}\left\{\left[(\boldsymbol{T}^e_{\rm unk})^{-1} - \boldsymbol{U}\right] + \frac{Z_{\rm unk}}{2Z_1}\boldsymbol{U} + \frac{Z_{\rm unk}}{2Z_2}\boldsymbol{U}\right\}, \tag{20}$$

$$\boldsymbol{T}^e_{\rm unk} - \boldsymbol{U} = \boldsymbol{K}^{-1}\boldsymbol{T}^c_{\rm unk}\boldsymbol{K}^{-1}, \tag{21}$$

$$(\boldsymbol{T}^c_{21})^{-1} = \frac{Z_1}{Z_{\rm unk}}\left\{\left[(\boldsymbol{T}^c_{\rm unk})^{-1} - \boldsymbol{U}\right] + \frac{Z_{\rm unk}}{2Z_1}\boldsymbol{U} + \frac{Z_{\rm unk}}{2Z_2}\boldsymbol{U}\right\}, \tag{22}$$

Then, inserting (15)–(18) into (20)–(22), the latter can be rewritten in terms of $\boldsymbol{Z}^c_{\rm unk}$ and $\boldsymbol{Z}^e_{\rm unk}$ as follows:

$$(\boldsymbol{T}^e_{21})^{-1} = \frac{Z_1}{Z_{\rm unk}}\left\{\boldsymbol{Z}_{||,{\rm unk}}(\boldsymbol{Z}^e_{\rm unk})^{-1} + \frac{Z_{\rm unk}}{2Z_1}\boldsymbol{U} + \frac{Z_{\rm unk}}{2Z_2}\boldsymbol{U}\right\}, \tag{23}$$

$$-\left[\boldsymbol{Z}^e_{\rm unk}(\boldsymbol{Z}_{||,\rm unk})^{-1}+\boldsymbol{U}\right]=\boldsymbol{K}\left[\boldsymbol{U}+\boldsymbol{Z}_{||,\rm unk}(\boldsymbol{Z}^c_{\rm unk})^{-1}\right]\boldsymbol{K}, \tag{24}$$

$$(\boldsymbol{T}^c_{21})^{-1}=\frac{Z_1}{Z_{\rm unk}}\left\{\boldsymbol{Z}_{||,\rm unk}(\boldsymbol{Z}^c_{\rm unk})^{-1}+\frac{Z_{\rm unk}}{2Z_1}\boldsymbol{U}+\frac{Z_{\rm unk}}{2Z_2}\boldsymbol{U}\right\}. \tag{25}$$

Next, based on (23) and (25), $\boldsymbol{Z}^e_{\rm unk}$ and $\boldsymbol{Z}^c_{\rm unk}$ can be represented in terms of $\boldsymbol{T}^e_{21}$ and $\boldsymbol{T}^c_{21}$ as follows:

$$(\boldsymbol{Z}^e_{\rm unk})^{-1}=\frac{1}{Z_1}\left[2(\boldsymbol{T}^e_{21})^{-1}-\boldsymbol{U}-\frac{Z_1}{Z_2}\boldsymbol{U}\right], \tag{26}$$

$$(\boldsymbol{Z}^c_{\rm unk})^{-1}=\frac{1}{Z_1}\left[2(\boldsymbol{T}^c_{21})^{-1}-\boldsymbol{U}-\frac{Z_1}{Z_2}\boldsymbol{U}\right], \tag{27}$$

respectively. Further, substituting (26) and (27) into (24) yields the relationship between $\boldsymbol{T}^e_{21}$ and $\boldsymbol{T}^c_{21}$ as follows:

$$-Z_1\left[2(\boldsymbol{T}^e_{21})^{-1}-\boldsymbol{U}-\frac{Z_1}{Z_2}\boldsymbol{U}\right]^{-1}(\boldsymbol{Z}_{P,\rm unk})^{-1}=\frac{\boldsymbol{K}\boldsymbol{Z}_{P,\rm unk}}{Z_1}\left[2(\boldsymbol{T}^c_{21})^{-1}-\boldsymbol{U}-\frac{Z_1}{Z_2}\boldsymbol{U}\right]\boldsymbol{K}, \tag{28}$$

where the equality $\boldsymbol{K}\boldsymbol{K}=-\boldsymbol{U}$ has been adopted in (28).

Finally, according to (11) and (13), $\boldsymbol{Z}^e_{21}$ and $\boldsymbol{Z}^c_{21}$ can be introduced to represent $\boldsymbol{T}^e_{21}$ and $\boldsymbol{T}^c_{21}$, respectively. Thereby, Eq. (28) can be expressed in terms of $\boldsymbol{Z}^e_{21}$ and $\boldsymbol{Z}^c_{21}$ as follows:

$$\begin{aligned}&-\left[2(\boldsymbol{t}_{21})^{-1}+2(\boldsymbol{t}_{21})^{-1}\boldsymbol{Z}_{P,21}(\boldsymbol{Z}^e_{21})^{-1}-\boldsymbol{U}-\frac{Z_1}{Z_2}\boldsymbol{U}\right]^{-1}(\boldsymbol{Z}_{P,\rm unk})^{-1}\\&=\frac{\boldsymbol{K}\boldsymbol{Z}_{P,\rm unk}}{Z_1^2}\left[2(\boldsymbol{t}_{21})^{-1}+2(\boldsymbol{t}_{21})^{-1}\boldsymbol{Z}_{P,21}(\boldsymbol{Z}^c_{21})^{-1}-\boldsymbol{U}-\frac{Z_1}{Z_2}\boldsymbol{U}\right]\boldsymbol{K}.\end{aligned} \tag{29}$$

Further, by simplifying (29), there will be the following expression:

$$\begin{gathered}-\frac{1}{4}\boldsymbol{Z}^e_{21}=\boldsymbol{K}\frac{\boldsymbol{Z}_{||,\rm unk}(\boldsymbol{t}_{21})^{-1}\boldsymbol{Z}_{||,21}}{Z_1}(\boldsymbol{Z}^c_{21})^{-1}\boldsymbol{K}\frac{\boldsymbol{Z}_{||,\rm unk}(\boldsymbol{t}_{21})^{-1}\boldsymbol{Z}_{||,21}}{Z_1},\\-\boldsymbol{K}^{-1}\boldsymbol{Z}^e_{21}\boldsymbol{K}^{-1}\boldsymbol{Z}^c_{21}=\frac{Z^2_{\rm unk}}{4}\boldsymbol{U},\end{gathered} \tag{30}$$

with

$$2(\boldsymbol{t}_{21})^{-1}=\left(\frac{Z_1}{Z_2}+1\right)\boldsymbol{U},\quad \frac{\boldsymbol{Z}_{||,\rm unk}(\boldsymbol{t}_{21})^{-1}\boldsymbol{Z}_{||,21}}{Z_1}=\frac{Z_{\rm unk}}{4}\boldsymbol{U}. \tag{31}$$

Eq. (30) gives the mathematical relationship between complementary metasurfaces in terms of their surface impedance matrices $\boldsymbol{Z}^e_{21}$ and $\boldsymbol{Z}^c_{21}$. Besides, Eq. (30) gives the mathematical relationship between complementary metasurfaces in terms of their surface impedance matrices $\boldsymbol{Z}^e_{21}$ and $\boldsymbol{Z}^c_{21}$. Eq. (30) can be also regarded as an extension of $Z^eZ^c=Z_0^2/4$ from complementary antennas to complementary metasurfaces.

3.3 The second model in terms of the surface impedance matrix

Similarly, the second model will be rewritten in terms of their surface impedance matrices $\boldsymbol{Z}^e_{21}$ and $\boldsymbol{Z}^c_{21}$. Firstly, by replacing the subscript "21" with "12" in (5), the following equation can be satisfied:

$$2Z_1^2(\boldsymbol{T}^c_{12})^{-1}=2\boldsymbol{Z}_{c,2}(\boldsymbol{T}^e_{12}-\boldsymbol{t}_{12})^{-1}\boldsymbol{Z}_{c,1}+(Z_1^2-Z_2^2)\boldsymbol{U}. \tag{32}$$

By adding (5) and (32), we can derive the following equation:

$$Z_2^2(\boldsymbol{T}^c_{21})^{-1}+Z_1^2(\boldsymbol{T}^c_{12})^{-1}=Z_1Z_2\boldsymbol{K}(\boldsymbol{T}^e_{21}-\boldsymbol{t}_{21})^{-1}\boldsymbol{K}+Z_1Z_2\boldsymbol{K}(\boldsymbol{T}^e_{12}-\boldsymbol{t}_{12})^{-1}\boldsymbol{K}. \tag{33}$$

Then, $\boldsymbol{Z}^e_{21}$ is inserted to simplify (33). Based on (12) and the equation $\boldsymbol{T}^e_{21}-\boldsymbol{t}_{12}=-\boldsymbol{Z}_{||,21}(\boldsymbol{Z}^e_{21}+\boldsymbol{Z}_{||,21})^{-1}\boldsymbol{t}_{12}$, Eq. (33) can be rewritten as follows:

$$Z_2^2(\boldsymbol{T}^c_{21})^{-1}+Z_1^2(\boldsymbol{T}^c_{12})^{-1}=-Z_1Z_2\boldsymbol{K}[(\boldsymbol{t}_{21})^{-1}+(\boldsymbol{t}_{12})^{-1}]\left(\boldsymbol{Z}^e_{21}\boldsymbol{Z}^{-1}_{||,21}+\boldsymbol{U}\right)\boldsymbol{K}, \tag{34}$$

where $\boldsymbol{Z}_{||,21} = \boldsymbol{Z}_{||,12}$ and $\boldsymbol{Z}^e_{21} = \boldsymbol{Z}^e_{12}$ have been adopted.

Next, the surface impedance matrix $\boldsymbol{Z}^c_{21}$ will be introduced for the complementary metasurface A^c. By substituting (13) and $\boldsymbol{T}^c_{12} = \boldsymbol{Z}^c_{21}(\boldsymbol{Z}^c_{21} + \boldsymbol{Z}_{||,21})^{-1}\boldsymbol{t}_{12}$ into (34), the latter will be simplified into the following equation:

$$\left[Z_2^2(\boldsymbol{t}_{21})^{-1} + Z_1^2(\boldsymbol{t}_{12})^{-1}\right]\left[\boldsymbol{U} + \boldsymbol{Z}_{||,21}(\boldsymbol{Z}^c_{21})^{-1}\right] = -Z_1Z_2\boldsymbol{K}\left[(\boldsymbol{t}_{21})^{-1} + (\boldsymbol{t}_{12})^{-1}\right]\left(\boldsymbol{Z}^e_{21}\boldsymbol{Z}^{-1}_{||,21} + \boldsymbol{U}\right)\boldsymbol{K}, \quad (35)$$

Finally, it can be easily verified that the following equations hold:

$$Z_2^2(\boldsymbol{t}_{21})^{-1} + Z_1^2(\boldsymbol{t}_{12})^{-1} = \frac{(Z_1+Z_2)^2}{2}\boldsymbol{U}, \quad (36)$$

$$Z_1Z_2\boldsymbol{K}\left[(\boldsymbol{t}_{21})^{-1} + (\boldsymbol{t}_{12})^{-1}\right] = \frac{(Z_1+Z_2)^2}{2}\boldsymbol{K}. \quad (37)$$

By substituting (36) and (37) into (35), the latter can be simplified as follows:

$$\left[\boldsymbol{U} + \boldsymbol{Z}_{||,21}(\boldsymbol{Z}^c_{21})^{-1}\right] = -\boldsymbol{K}\left(\boldsymbol{Z}^e_{21}\boldsymbol{Z}^{-1}_{||,21} + \boldsymbol{U}\right)\boldsymbol{K}. \quad (38)$$

Further, based on (8) and the equality $-\boldsymbol{K}\boldsymbol{K} = \boldsymbol{U}$, Eq. (38) can be simplified as follows:

$$-\boldsymbol{K}\boldsymbol{Z}^e_{21}\boldsymbol{K}\boldsymbol{Z}^c_{21} = \boldsymbol{Z}_{||,21}\boldsymbol{Z}_{||,21}. \quad (39)$$

Similar to (30), Eq. (39) provides another expression of two complementary metasurfaces in terms of their surface impedance matrices $\boldsymbol{Z}^e_{21}$ and $\boldsymbol{Z}^c_{21}$.

3.4 Solution of the relative permittivity

In this part, these two theoretical models will be combined together to solve the unknown relative permittivity $\epsilon_{r,\mathrm{unk}}$. Since (30) and (39) both establish the mathematical relationship for complementary metasurfaces in terms of their surface impedance matrices at normal incidence, they should be consistent with each other due to unique reflection and transmission characteristics of the metasurface. By comparing (30) and (39), the following equation will be satisfied at normal incidence:

$$\boldsymbol{K}^{-1}\boldsymbol{Z}^e_{21}\boldsymbol{K}\boldsymbol{Z}^c_{21} = \boldsymbol{Z}_{||,21}\boldsymbol{Z}_{||,21} = \frac{Z^2_{\mathrm{unk}}}{4}\boldsymbol{U}, \quad (40)$$

where Eq. (8) and the equality $-\boldsymbol{K}\boldsymbol{K} = \boldsymbol{U}$ have been adopted in (40). Finally, the wave impedance Z_{unk} and relative permittivity $\epsilon_{r,\mathrm{unk}}$ are given by

$$Z_{\mathrm{unk}} = \frac{2Z_1Z_2}{Z_1+Z_2}, \quad \sqrt{\epsilon_{r,\mathrm{unk}}} = \frac{\sqrt{\epsilon_{r,1}} + \sqrt{\epsilon_{r,2}}}{2}, \quad (41)$$

where Z_{unk} is the corresponding wave impedance of $\epsilon_{r,\mathrm{unk}}$. Especially, Z_{unk} is not the surface impedance matrix of the metasurface. In fact, it should be nearly impossible to find an analytical expression of the surface impedance matrix for all metasurfaces. Different metasurfaces will have different electromagnetic characteristics, so that the boundary condition (surface impedance matrix) will be strongly related to the geometrical structure and parameters of metasurfaces. Thus, the analytical expression of (41) cannot correspond to surface impedance matrix of metasurfaces.

It should be noted that Eq. (41) is not completely accurate due to the deviation of the modified Babinet's principle whose error gradually increases as the incidence angle increases. Thereby, the mathematical derivation of (41) is only conducted at normal incidence to reduce the error. According to the analysis, the expression of $Z_{\mathrm{unk}} = \frac{2Z_1Z_2}{Z_1+Z_2}$ in (41) should be approximately related to the secondary radiation of the average surface current density on the metasurface. Specifically, when the metasurface on the substrate interface can be regarded as embedded into a zero-thickness homogenized dielectric layer with a specific relative permittivity $\epsilon_{r,\mathrm{unk}}$. Further, due to the sub-wavelength periodicity of the meta-atoms, the average surface current density (i.e., zero-order Floquet's mode) should be considered mainly. Since the induced current on the metasurface is almost unchanged in the two cases, the electromagnetic waves with the same energy will be radiated from the metasurface. Finally, according to the transmission line theory, the average surface current density can be regarded as a kind of current source and radiates waves into both sides of the metasurface, and Eq. (41) indicates the equal output impedances, i.e., $Z_{\mathrm{unk}}||Z_{\mathrm{unk}} = Z_1||Z_2$.

4 Verification

4.1 Verification at arbitrary incidence

Although the mathematical derivation of (41) is only conducted at normal incidence, it is reasonable to speculate that the relative permittivity, as an inherent electrical parameter, should be independent of the incidence angle. Thereby, Eq. (41) should also hold at arbitrary oblique incidence. To this end, Eq. (1) at normal incidence needs to be rewritten at oblique incidence. Specifically, at oblique incidence with the tangential incident field $\boldsymbol{E}_{\text{inc}}^{\tan}$ and transmitted field $\boldsymbol{E}_{\text{tra}}^{\tan}$, Eq. (1) can be generally expressed as follows [38]:

$$(\boldsymbol{T}_{21}^{e,\tan})^{-1} = (\boldsymbol{t}_{\text{unk},1}^{\tan})^{-1}\boldsymbol{t}_{1,\text{unk}}^{\tan}\left[(\boldsymbol{T}_{\text{unk}}^{e,\tan})^{-1} - 2\boldsymbol{U} + (\boldsymbol{t}_{1,\text{unk}}^{\tan})^{-1} + (\boldsymbol{t}_{2,\text{unk}}^{\tan})^{-1}\right], \tag{42}$$

with

$$\begin{aligned}
\boldsymbol{t}_{\text{unk},1}^{(11)} &= \frac{2Z_{\text{unk}}\cos\theta_{\text{unk}}}{Z_{\text{unk}}\cos\theta_{\text{unk}} + Z_1\cos\theta_1},\\
\boldsymbol{t}_{\text{unk},1}^{(22)} &= \frac{2Z_{\text{unk}}/\cos\theta_{\text{unk}}}{Z_{\text{unk}}/\cos\theta_{\text{unk}} + Z_1/\cos\theta_1},\\
\boldsymbol{t}_{\text{unk},1}^{\tan} &= \begin{bmatrix} \boldsymbol{t}_{\text{unk},1}^{(11)} & 0 \\ 0 & \boldsymbol{t}_{\text{unk},1}^{(22)} \end{bmatrix},\\
\begin{bmatrix} E_{\text{tra}}^{\text{TM}}\cos\theta_2 \\ E_{\text{tra}}^{\text{TE}} \end{bmatrix} &= \boldsymbol{T}_{21}^{e,\tan}\begin{bmatrix} E_{\text{inc}}^{\text{TM}}\cos\theta_1 \\ E_{\text{inc}}^{\text{TE}} \end{bmatrix},
\end{aligned} \tag{43}$$

where the TM (TE) indicates that the electrical field is parallel (perpendicular) with respect to the incidence plane; $t_{\text{unk},1}^{(11)}$ and $t_{\text{unk},1}^{(22)}$ are the tangential transmission matrices for the TM and TE waves resulted from the existing Fresnel' formulas, respectively; and other tangential transmission matrices like $\boldsymbol{t}_{1,\text{unk}}^{\tan}$ and $\boldsymbol{t}_{2,\text{unk}}^{\tan}$ can be defined similarly as $\boldsymbol{t}_{\text{unk},1}^{\tan}$.

Eq. (42) will be adopted to verify the proposed theory for the specific metasurface A^e by comparing simulated and theoretical reflection matrices $\boldsymbol{R}_{21}^{e}(\boldsymbol{T}_{21}^{e,\tan})$ through the simulated reflection matrix $\boldsymbol{R}_{\text{unk}}^{e}(\boldsymbol{T}_{\text{unk}}^{e,\tan})$. Specifically, as shown in Figure 3, we can derive $\boldsymbol{T}_{\text{unk}}^{e,\tan}$ beforehand through full-wave simulation as follows:

$$\boldsymbol{T}_{\text{unk}}^{e,\tan} = \boldsymbol{R}_{\text{unk}}^{e,\tan} + \boldsymbol{U}, \tag{44}$$

$$\boldsymbol{R}_{\text{unk}}^{e,\tan} = \begin{bmatrix} R_{\text{unk}}^{\text{TM-TM}} & R_{\text{unk}}^{\text{TM-TE}}\cos\theta_{\text{unk}} \\ R_{\text{unk}}^{\text{TE-TM}}/\cos\theta_{\text{unk}} & R_{\text{unk}}^{\text{TE-TE}} \end{bmatrix}, \quad \boldsymbol{R}_{\text{unk}}^{e} = \begin{bmatrix} R_{\text{unk}}^{\text{TM-TM}} & R_{\text{unk}}^{\text{TM-TE}} \\ R_{\text{unk}}^{\text{TE-TM}} & R_{\text{unk}}^{\text{TE-TE}} \end{bmatrix}, \tag{45}$$

where $\boldsymbol{R}_{\text{unk}}^{e}$ is the simulated reflection matrix for the metasurface A^e (due to the existence of the radiation boundary condition in the HFSS (high frequency structure simulator) simulation, the simulated transmission matrix will be invalid); $\boldsymbol{R}_{\text{unk}}^{e,\tan}$ is the tangential reflection matrix for A^e, and Eq. (44) is based on the continuity condition of the tangential electrical field; θ_{unk} is the incidence angle in the homogenized dielectric with the relative permittivity $\epsilon_{r,\text{unk}}$, and satisfies the refraction law, i.e.,$\sqrt{\epsilon_{r,1}}\sin\theta_1 = \sqrt{\epsilon_{r,2}}\sin\theta_2 = \sqrt{\epsilon_{r,\text{unk}}}\sin\theta_{\text{unk}}$. After determining $\boldsymbol{T}_{\text{unk}}^{e,\tan}$, the theoretical $\boldsymbol{T}_{21}^{e,\tan}$ can be directly solved through (42) for the metasurface in a dielectric half-space. Finally, $\boldsymbol{T}_{21}^{e,\tan}$ can be similarly converted into the following theoretical reflection matrix $\boldsymbol{R}_{21}^{e}$ for comparison with the simulated ones:

$$\boldsymbol{T}_{21}^{e,\tan} = \boldsymbol{R}_{21}^{e,\tan} + \boldsymbol{U}, \tag{46}$$

$$\boldsymbol{R}_{21}^{e,\tan} = \begin{bmatrix} R_{21}^{\text{TM-TM}} & R_{21}^{\text{TM-TE}}\cos\theta_1 \\ R_{21}^{\text{TE-TM}}/\cos\theta_1 & R_{21}^{\text{TE-TE}} \end{bmatrix}, \quad \boldsymbol{R}_{21}^{e} = \begin{bmatrix} R_{21}^{\text{TM-TM}} & R_{21}^{\text{TM-TE}} \\ R_{21}^{\text{TE-TM}} & R_{21}^{\text{TE-TE}} \end{bmatrix}. \tag{47}$$

Finally, the consistence between the simulated $\boldsymbol{R}_{21}^{e}$ and calculated $\boldsymbol{R}_{21}^{e}$ (from $\boldsymbol{R}_{\text{unk}}^{e}$) will support the proposed theory. Thereby, the derived $\epsilon_{r,\text{unk}}$ can have the problem of metasurface in a dielectric half-space transformed into another problem of the same metasurface in a homogenized dielectric, which can be applied to reduce the difficulty in solving the metasurface's boundary condition.

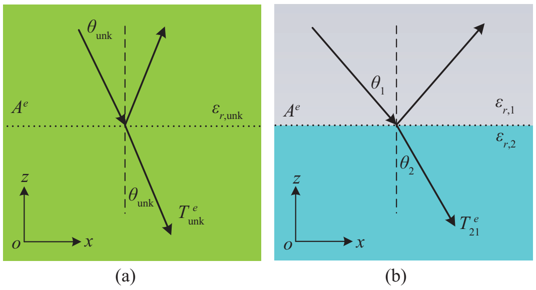

Figure 3 (Color online) Model applied to verify the proposed theory. (a) Metasurface represented by black dotted lines in the homogenized dielectric with the relative permittivity $\epsilon_{r,\text{unk}}$ and (b) the same metasurface black dotted lines in a dielectric half-space.

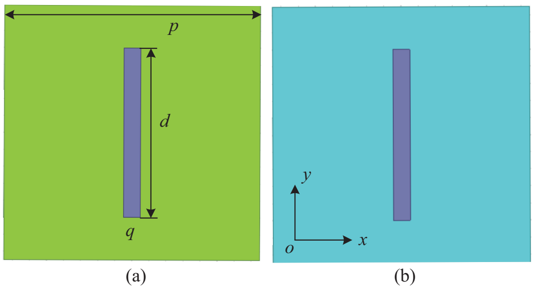

Figure 4 (Color online) Isotropic metasurface without polarization conversion (a) in a homogenized dielectric with the relative permittivity $\epsilon_{r,\text{unk}}$ and (b) in a dielectric half-space with the relative permittivities $\epsilon_{r,1}$ and $\epsilon_{r,2}$.

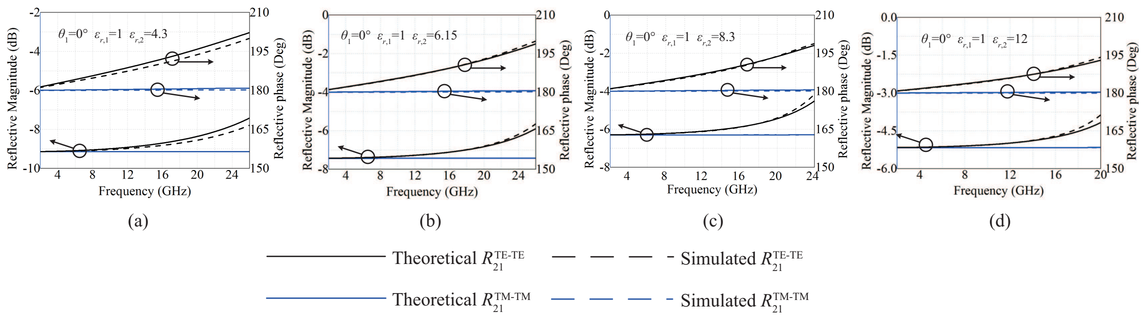

Figure 5 (Color online) Theoretical and simulated reflection coefficients for the metasurface in a dielectric half-space at normal incidence with (a) $\epsilon_{r,2} = 4.3$, (b) $\epsilon_{r,2} = 6.15$, (c) $\epsilon_{r,2} = 8.3$, and (d) $\epsilon_{r,2} = 12$.

4.2 Isotropic metasurface at arbitrary incidence

As shown in Figure 4, the unit cell of a metasurface is given with geometric parameters of $p = 3$ mm, $d = 2$ mm, and $q = 0.2$ mm. The commercial software HFSS is applied to verify the proposed theory. In the simulation, the x- and y-directed boundaries of the unit cell are set to be periodic, and the radiation boundary condition is adopted to avoid multiple reflections and refractions. Besides, in order to ensure the simulation accuracy, the maximum error of the reflection (transmission) coefficients is set to be 0.005, and the adaptive mesh refinement in the HFSS is adopted to achieve a better mesh for the given metasurface.

Figure 5 shows the theoretical and simulated reflection matrices $\boldsymbol{R}_{21}^{e}$ for the isotropic metasurface in a dielectric half-space. For convenience without loss of generality, the dielectric 1 is set as air ($\epsilon_{r,1} = 1$), while the relative permittivity $\epsilon_{r,2}$ is set as a varying parameter. Since there is no polarization conversion, only the co-polarized reflection coefficients $R_{21}^{\text{TM-TM}}$ and $R_{21}^{\text{TE-TE}}$ are considered. When the relative permittivity $\epsilon_{r,2}$ varies from 4.3 to 12.0, the theoretical results including reflective magnitude and phase match well to the simulated ones, regardless of the relative permittivity $\epsilon_{r,2}$. Especially, due to the cut-line's much smaller dimension in the x-direction, there is almost no induced current for x-polarized wave (i.e., the TM wave at normal incidence), which corresponds to the case of no metasurface. Thereby, the x-polarized reflection coefficient can be theoretically solved as $R_{21}^{\text{TM-TM}}|_{\theta_1=0^\circ} = \frac{Z_2-Z_1}{Z_2+Z_1}$, which conforms to the simulation.

Further, Figure 6 shows the theoretical and simulated reflection matrices at oblique incidence for the metasurface in a dielectric half-space. It is observed that, when the relative permittivity $\epsilon_{r,2}$ is fixed as 6.15 and incidence angle θ_1 varies from 15° to 85°, there is still a good agreement between theoretical and simulated reflection coefficients including reflective magnitude and phase. Similarly, there is almost no induced current on metallic cut-line under the TM oblique incidence, so the TM reflection coefficient can be theoretically solved as $R_{21}^{\text{TM-TM}} = \frac{Z_2 \cos\theta_2 - Z_1 \cos\theta_1}{Z_2 \cos\theta_2 + Z_1 \cos\theta_1}$ according to the existing Fresnel's formulas, which also conforms to the simulation. Thus, the simulations not only validate $\epsilon_{r,\text{unk}}$ at oblique incidence, but also support the proposed theory that the problem of the metasurface in a dielectric half-space can be transformed into a simpler problem of the same metasurface in a homogenized dielectric with the relative

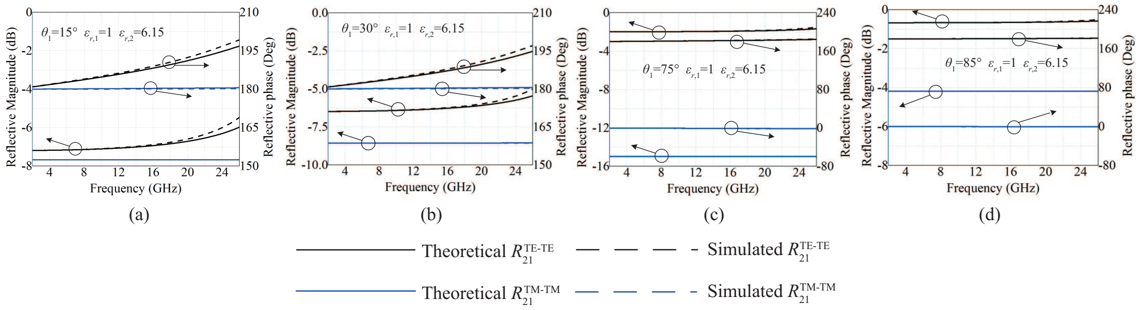

Figure 6 (Color online) Theoretical and simulated reflection coefficients for metasurface in a dielectric half-space at oblique incidence with fixed $\epsilon_{r,2} = 6.15$. (a) $\theta_1 = 15^\circ$; (b) $\theta_1 = 30^\circ$; (c) $\theta_1 = 75^\circ$; (d) $\theta_1 = 85^\circ$.

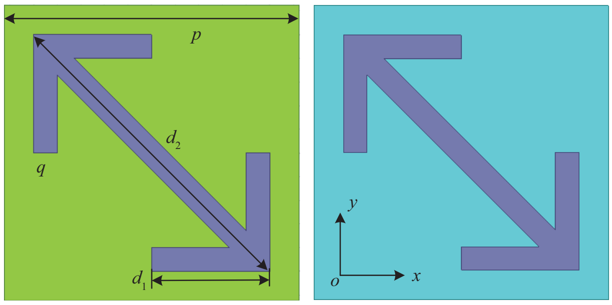

(a) (b)

Figure 7 (Color online) Anisotropic metasurface with polarization conversion in (a) a homogenized dielectric and (b) a dielectric half-space.

permittivity $\epsilon_{r,\text{unk}}$.

Besides, it should be noted that the operation frequency of the proposed theory is strongly related to the periodicity of the meta-atoms and the relative permittivity of the dielectric half-space. The main reason is that the metasurface is handled as a homogenized surface with an average boundary condition (i.e., surface impedance matrix), which requests that the periodicity of the meta-atoms needs to be much smaller than the operation wavelength (i.e., zero-order Floquet's mode [41, 42]). Otherwise, high-order Floquet's modes will influence the accuracy of the average boundary condition (i.e., surface impedance matrix). Finally, considering that the theoretical magnitude and phase are the almost same as those of the simulated ones, it can be concluded that the simulation supports the proposed theory at normal incidence.

4.3 Anisotropic metasurface at arbitrary incidence

In order to increase the credibility of the proposed theory, a second meta-atom (cf. Figure 7) is given. The geometric parameters of the unit cell are $p = 2.5$ mm, $d_1 = 1$ mm, $d_2 = 2\sqrt{2}$ mm, and $q = 0.2$ mm. Different from the metasurface in Subsection 4.2, the presented metasurface can result in cross-polarized secondary re-radiated wave in the dielectric half-space. Finally, a similar simulation procedure will be conducted to verify the proposed theory.

Figure 8 shows the theoretical and simulated reflection matrices for the anisotropic metasurface in a dielectric half-space at normal incidence ($\theta_1 = 0^\circ$). Similar to the previous example, the dielectric 1 is set as air ($\epsilon_{r,1} = 1$), while the relative permittivity of dielectric 2 is set as a varying parameter. Due to the structure symmetry and reciprocity principle, there will be the equations $R_{21}^{\text{TM-TM}}|_{\theta_1=0^\circ} = R_{21}^{\text{TE-TE}}|_{\theta_1=0^\circ}$ and $R_{21}^{\text{TE-TM}} = R_{21}^{\text{TM-TE}}$, so that only $R_{21}^{\text{TE-TE}}$ and $R_{21}^{\text{TE-TM}}$ are plotted in Figure 8. It can be found that the theoretical results including reflective magnitude and phase match well with the simulated ones, regardless of the $\epsilon_{r,2}$ and polarization status. Especially, as $\left|R_{21}^{\text{TE-TM}}\right|$ varies from -38 to -10 dB and $\angle R_{21}^{\text{TE-TM}}$ varies from 90° to -120° in Figure 8(d), the theoretical results still conform to the simulated ones, demonstrating high accuracy of the proposed theory. Thus, it can be concluded that the proposed theory holds at normal incidence for the anisotropic metasurface.

Figure 9 shows the theoretical and simulated reflection matrices at oblique incidence. The relative permittivity of dielectric 2 is fixed as $\epsilon_{r,2} = 4.6$, while the incidence angle varies from 20° to 80°.

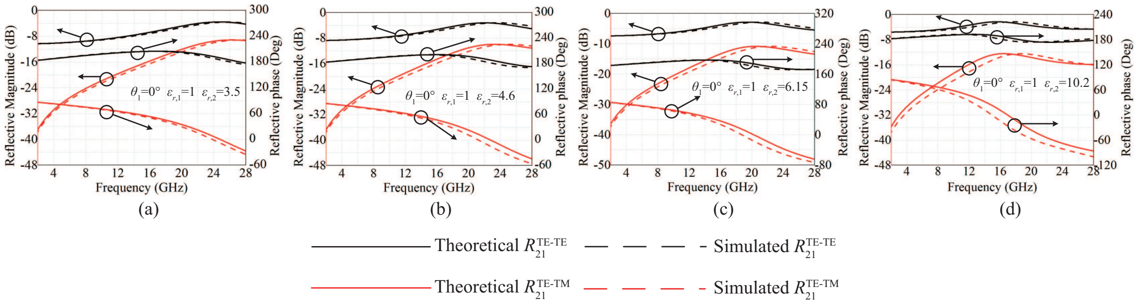

Figure 8 (Color online) Theoretical and simulated reflection coefficients of a metasurface in a dielectric half-space at normal incidence with varying dielectric 2. (a) $\epsilon_{r,2} = 3.5$; (b) $\epsilon_{r,2} = 4.6$; (c) $\epsilon_{r,2} = 6.15$; (d) $\epsilon_{r,2} = 10.2$.

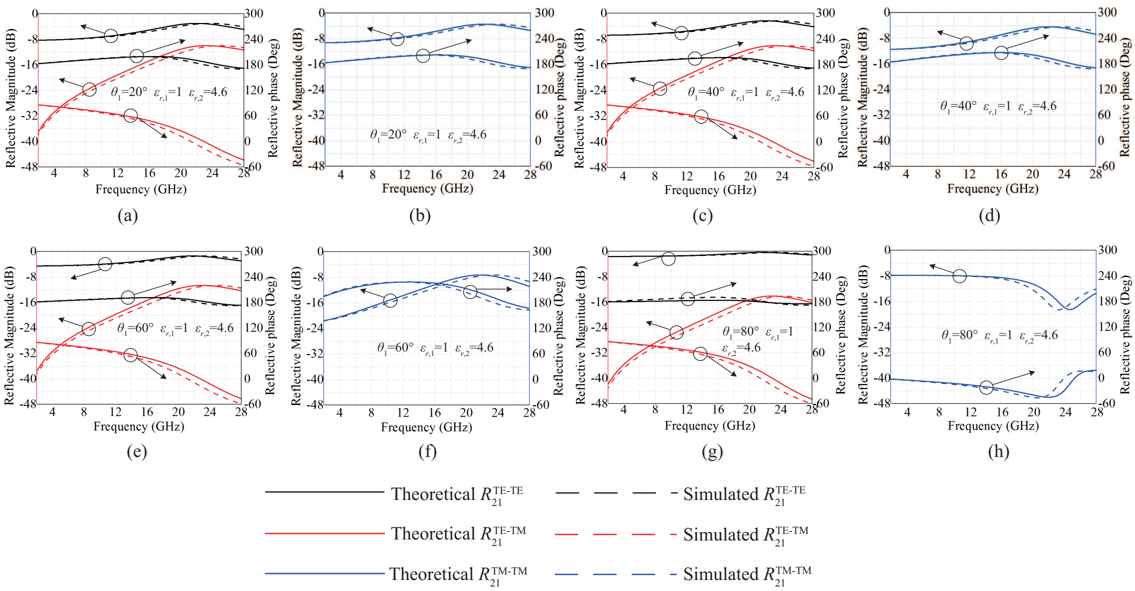

Figure 9 (Color online) Theoretical and simulated reflection coefficients of a metasurface in a dielectric half-space at oblique incidence with fixed $\epsilon_{r,2} = 4.6$. $R_{21}^{\text{TE-TE}}$ and $R_{21}^{\text{TE-TM}}$ at (a) $\theta_1 = 20^\circ$, (c) $\theta_1 = 40^\circ$, (e) $\theta_1 = 60^\circ$, and (g) $\theta_1 = 80^\circ$. $R_{21}^{\text{TM-TM}}$ at (b) $\theta_1 = 20^\circ$, (d) $\theta_1 = 40^\circ$, (f) $\theta_1 = 60^\circ$, and (h) $\theta_1 = 80^\circ$.

Since the metasurface is no longer symmetrical at oblique incidence, so that the co-polarized reflection coefficients are unequal, i.e., $R_{21}^{\text{TM-TM}} \neq R_{21}^{\text{TE-TE}}$. Nevertheless, the theoretical results still conform to the simulated ones, regardless of the polarization status and incidence angle. The consistency supports the proposed theory at oblique incidence again that the metasurface in a dielectric half-space can be transformed into the same metasurface in a homogenized dielectric with the relative permittivity $\epsilon_{r,\text{unk}}$.

Besides, it is also noted that there is a little error, especially for $R_{21}^{\text{TM-TM}}$ at $\theta_1 = 80^\circ$ in Figure 9(h). According to the analysis, the discrepancy can be explained by the following three aspects. Firstly, the proposed theory is based on the solution of the tangential fields. It can be easily found that the discrepancy obviously occurs with the resonance of the metasurface at $\theta_1 = 80^\circ$. In this case, the reflected TM wave shows much less tangential component than the case of no metasurface (cf. Figure 6(d)), which results in inevitable errors. Secondly, the derived $\epsilon_{r,\text{unk}}$ is not completely accurate. In the proposed theory, $\epsilon_{r,\text{unk}}$ is derived based on two kinds of Babinet's principle. However, it is previously shown that there is a little error for the second modified Babinet principle. Finally, as discussed in Subsection 4.2, the metasurface needs to be handled as a homogenized surface with an average boundary condition (i.e., zero-order Floquet's mode [41, 42]). At larger incidence angle, the high-order Floquet's modes with tangential wave number $k_{||} = k_0 \sin\theta_1 + \frac{2\pi m}{p}$ will have more influence on the accuracy of the average boundary condition.

5 Conclusion

In conclusion, we transform the problem of a metasurface in a dielectric half-space into another simpler problem of the same metasurface in a homogenized dielectric space with relative permittivity $\epsilon_{r,\mathrm{unk}}$. First, two kinds of Babinet's principles (models) are given for complementary metasurfaces in a dielectric half-space. One of the models including a specific yet unknown relative permittivity $\epsilon_{r,\mathrm{unk}}$ can realize the above transformation. Then, due to their complex mathematical forms in terms of the transmission matrix, the surface impedance matrix is also introduced to simplify the two models. Next, by comparing these two theoretical models with each other, the specific relative permittivity $\epsilon_{r,\mathrm{unk}}$ is analytically derived as $\sqrt{\epsilon_{r,\mathrm{unk}}} = \sqrt{\epsilon_{r,1}}/2 + \sqrt{\epsilon_{r,2}}/2$. Finally, two different kinds of metasurfaces are given to verify the theory. Thanks to the proposed theory, only the metasurface in the homogenized dielectric needs to be considered, so that the analysis and design of the metasurface can be greatly simplified.

Acknowledgements This work was supported by National Natural Science Foundation of China (Grants Nos. 62101428, 62171362), Postdoctoral Science Foundation of China (Grant No. 2021M692530), and Fundamental Research Funds for the Central Universities (Grant No. xzy012022089).

References

1 Yu N, Capasso F. Flat optics with designer metasurfaces. Nat Mater, 2014, 13: 139–150
2 Liang Y C, Chen J, Long R, et al. Reconfigurable intelligent surfaces for smart wireless environments: channel estimation, system design and applications in 6G networks. Sci China Inf Sci, 2021, 64: 200301
3 Mutlu M, Ozbay E. A transparent 90° polarization rotator by combining chirality and electromagnetic wave tunneling. Appl Phys Lett, 2012, 100: 051909
4 Farmahini-Farahani M, Mosallaei H. Birefringent reflectarray metasurface for beam engineering in infrared. Opt Lett, 2013, 38: 462
5 Pfeiffer C, Zhang C, Ray V, et al. High performance bianisotropic metasurfaces: asymmetric transmission of light. Phys Rev Lett, 2014, 113: 023902
6 Ma H F, Wang G Z, Kong G S, et al. Broadband circular and linear polarization conversions realized by thin birefringent reflective metasurfaces. Opt Mater Express, 2014, 4: 1717–1724
7 Luo Z J, Ren X Y, Wang Q, et al. Anisotropic and nonlinear metasurface for multiple functions. Sci China Inf Sci, 2021, 64: 192301
8 Ghosh S, Ghosh J, Singh M S, et al. A low-profile multifunctional metasurface reflector for multiband polarization transformation. IEEE Trans Circ Syst II, 2023, 70: 76–80
9 Ortiz J D, Baena J D, Losada V, et al. Self-complementary metasurface for designing narrow band pass/stop filters. IEEE Microw Wireless Compon Lett, 2013, 23: 291–293
10 Born N, Reuter M, Koch M, et al. High-Q terahertz bandpass filters based on coherently interfering metasurface reflections. Opt Lett, 2013, 38: 908–910
11 Reddy M A, Pandeeswari R, Ko S B. Non-bianisotropic complementary split ring resonator metamaterial bandstop filter using cylindrical metal vias. IEEE Trans Circ Syst II, 2023, 70: 959–963
12 Li A, Kim S, Luo Y, et al. High-power transistor-based tunable and switchable metasurface absorber. IEEE Trans Microwave Theor Techn, 2017, 65: 2810–2818
13 Zhou Z H, Chen K, Zhao J M, et al. Metasurface Salisbury screen: achieving ultra-wideband microwave absorption. Opt Express, 2017, 25: 30241
14 Shuang Y, Zhao H T, Wei M L, et al. One-bit quantization is good for programmable coding metasurfaces. Sci China Inf Sci, 2022, 65: 172301
15 Chen W J, Chen R, Zhou Y, et al. A switchable metasurface between meta-lens and absorber. IEEE Photon Technol Lett, 2019, 31: 1187–1190
16 Rabinovich O, Epstein A. Dual-polarized all-metallic metagratings for perfect anomalous reflection. Phys Rev Appl, 2020, 14: 64028
17 Xu G, Hum S V, Eleftheriades G V. Dual-band reflective metagratings with interleaved meta-wires. IEEE Trans Antenn Propag, 2021, 69: 2181–2193
18 Lee S G, Lee J H. Azimuthal six-channel retrodirective metagrating. IEEE Trans Antenn Propag, 2021, 69: 3588–3592
19 Popov V, Boust F, Burokur S N. Controlling diffraction patterns with metagratings. Phys Rev Appl, 2018, 10: 11002
20 Casolaro A, Toscano A, Alu A, et al. Dynamic beam steering with reconfigurable metagratings. IEEE Trans Antenn Propag, 2020, 68: 1542–1552
21 Wang Y F, Ge Y H, Chen Z Z, et al. Broadband high-efficiency ultrathin metasurfaces with simultaneous independent control of transmission and reflection amplitudes and phases. IEEE Trans Microwave Theor Techn, 2022, 70: 254–263
22 Gao X, Han X, Cao W P, et al. Ultrawideband and high-efficiency linear polarization converter based on double V-shaped metasurface. IEEE Trans Antenn Propag, 2015, 63: 3522–3530
23 Fang C, Cheng Y Z, He Z Q, et al. A broadband reflective linear polarization converter based on multi-reflection interference theory. In: Proceedings of Progress In Electromagnetic Research Symposium (PIERS), 2016. 3033–3036
24 Whitbourn L B, Compton R C. Equivalent-circuit formulas for metal grid reflectors at a dielectric boundary. Appl Opt, 1985, 24: 217–220
25 Jiang S C, Xiong X, Hu Y S, et al. Controlling the polarization state of light with a dispersion-free metastructure. Phys Rev X, 2014, 4: 021026
26 Liu X B, Zhang J S, Li W, et al. An analytical design of cross polarization converter based on the gangbuster metasurface. Antenn Wirel Propag Lett, 2017, 16: 1028–1031
27 Liu X B, Li W, Zhao Z Z, et al. Tangential network transmission theory of reflective metasurface with obliquely incident plane waves. IEEE Trans Microwave Theor Techn, 2018, 66: 64–72
28 Compton R C, Whitbourn L B, McPhedran R C. Strip gratings at a dielectric interface and application of Babinet's principle. Appl Opt, 1984, 23: 3236–3242

29 Tretyakov S A. Analytical Modeling in Applied Electromagnetics. Norwood: Artech House, 2003
30 Kuester E F, Mohamed M A, Piket-May M, et al. Averaged transition conditions for electromagnetic fields at a metafilm. IEEE Trans Antenn Propag, 2003, 51: 2641–2651
31 Luukkonen O, Simovski C, Granet G, et al. Simple and accurate analytical model of planar grids and high-impedance surfaces comprising metal strips or patches. IEEE Trans Antenn Propag, 2008, 56: 1624–1632
32 Padooru Y R, Yakovlev A B, Chen P Y, et al. Analytical modeling of conformal mantle cloaks for cylindrical objects using sub-wavelength printed and slotted arrays. J Appl Phys, 2012, 112:
33 Holloway C L, Kuester E F. A homogenization technique for obtaining generalized sheet-transition conditions for a metafilm embedded in a magnetodielectric interface. IEEE Trans Antenn Propag, 2016, 64: 4671–4686
34 Moeini S. Homogenization of fractal metasurface based on extension of Babinet-booker's principle. Antennas Wirel Propag Lett, 2019, 18: 1061–1065
35 Ney M M. Method of moments as applied to electromagnetic problems. IEEE Trans Microwave Theor Techn, 1985, 33: 972–980
36 Harriton R F. Field Computation by Moment Methods. Hoboken: Wiley-IEEE Press, 1993
37 Pendry J B, Holden A J, Stewart W J, et al. Extremely low frequency plasmons in metallic mesostructures. Phys Rev Lett, 1996, 76: 4773–4776
38 Liu X B, Zhang J S, Chen X M, et al. A generalized accurate model for complementary periodic subwavelength metasurface based on Babinet principle. IEEE Trans Antenn Propag, 2020, 68: 3780–3790
39 Liu X B, Xue W, Chen X M, et al. On the uniqueness of virtual substrate for metasurface in a dielectric half-space. Sci China Inf Sci, 2021, 65: 112302
40 Liu X B, Lu R, Zhu S T, et al. Analysis of complementary metasurfaces based on the Babinet principle. IEEE Microw Wireless Compon Lett, 2019, 29: 8–10
41 Xiao S Y, He Q, Qu C, et al. Mode-expansion theory for inhomogeneous meta-surfaces. Opt Express, 2013, 21: 27219–27237
42 Munk B A. Frequency Selective Surfaces: Theory and Design. Hoboken: Wiley Press, 2000